Inorg. Chem. **2008**, *47*, 11228−11236

Properties of Square-Pyramidal Alkyl−Thiolate Fe^{III} Complexes, Including an Analogue of the Unmodified Form of Nitrile Hydratase

Priscilla Lugo-Mas, Wendy Taylor, Dirk Schweitzer, Roslyn M. Theisen, Liang Xu, Jason Shearer, Rodney D. Swartz, Morgan C. Gleaves, Antonio DiPasquale,† Werner Kaminsky,† and Julie A. Kovacs*

The Department of Chemistry, University of Washington, Box 351700 Seattle, Washington 98195-1700

Received September 4, 2008

The syntheses and structures of three new coordinatively unsaturated, monomeric, square-pyramidal thiolate-ligated Fe(III) complexes are described, $[Fe^{III}((tame\text{-}N_3)S_2^{Me2})]^+$ (**1**), $[Fe^{III}(Et\text{-}N_2S_2^{Me2})(py)]^{1-}$ (**3**), and $[Fe^{III}((tame\text{-}N_2S)S_2^{Me2})]^{2-}$ (**15**). The anionic bis-carboxamide, tris-thiolate N_2S_3 coordination sphere of **15** is potentially similar to that of the yet-to-be characterized unmodified form of NHase. Comparison of the magnetic and reactivity properties of these reveals how anionic charge build up (from cationic **1** to anionic **3** and dianionic **15**) and spin-state influence apical ligand affinity. For all of the ligand-field combinations examined, an intermediate $S = 3/2$ spin state was shown to be favored by a strong N_2S_2 basal plane ligand field, and this was found to reduce the affinity for apical ligands, even when they are built in. This is in contrast to the post-translationally modified NHase active site, which is low spin and displays a higher affinity for apical ligands. Cationic **1** and its reduced Fe^{II} precursor are shown to bind NO and CO, respectively, to afford $[Fe^{III}((tame\text{-}N_3)S_2^{Me})(NO)]^+$ (**18**, $\nu_{NO} = 1865\ cm^{-1}$), an analogue of NO-inactivated NHase, and $[Fe^{II}((tame\text{-}N_3)S_2^{Me})(CO)]$ (**16**; ν_{CO} stretch (1895 cm^{-1}). Anions (N_3^-, CN^-) are shown to be unreactive toward **1**, **3**, and **15** and neutral ligands unreactive toward **3** and **15**, even when present in 100-fold excess and at low temperatures. The curtailed reactivity of **15**, an analogue of the unmodified form of NHase, and its apical-oxygenated $S = 3/2$ derivative $[Fe^{III}((tame\text{-}N_2SO_2)S_2^{Me2})]^{2-}$ (**20**) suggests that regioselective post-translational oxygenation of the basal plane NHase cysteinate sulfurs plays an important role in promoting substrate binding. This is supported by previously reported theoretical (DFT) calculations.[1]

Introduction

Nitrile hydratases (NHases) are nonheme iron enzymes that catalyze the enantioselective hydrolysis of nitriles to amides.[2−6] The active sites of NHases are unusual and differ dramatically from the majority of nonheme iron enzymes in that they contain three cysteinate ligands and two deprotonated peptide amides[7,8] as opposed to the more typical N/O ($N_2^{His}O^{Asp,Glu}$ facial triad) ligand environment.[9−12] The more covalent and electron-rich ligand environment of NHase stabilizes low-spin ($S = 1/2$) iron in the +3 oxidation state.[13,14] Two of the cysteinates are oxidized (post-translationally modified): one to a sulfenic

* To whom correspondence should be addressed. Phone: (206)543-0713. Fax: (206)685-8665. E-mail: kovacs@chem.washington.edu.
† UW staff crystallographers.

(1) Dey, A.; Chow, M.; Taniguchi, K.; Lugo-Mas, P.; Davin, S. D.; Maeda, M.; Kovacs, J. A.; Odaka, M.; Hedman, B.; Hodgson, K. O.; Solomon, E. I. *J. Am. Chem. Soc.* **2006**, *128*, 533–541.
(2) Mitra, S.; Holz, R. C. *J. Biol. Chem.* **2007**, *282*, 7397–7404.
(3) Noguchi, T.; Nojiri, M.; Takei, K.; Odaka, M.; Kamiya, N. *Biochemistry* **2003**, *42*, 11642–11650.
(4) Kobayashi, M.; Shimizu, S. *Nat. Biotechnol.* **1998**, *16*, 733–736.
(5) Sugiura, Y.; Kuwahara, J.; Nagasawa, T.; Yamada, H. *J. Am. Chem. Soc.* **1987**, *109*, 5848–5850.
(6) Stolz, A.; Trott, S.; Binder, M.; Bauer, R.; Hirrlinger, B.; Layh, N.; Knackmuss, H.-J. *J. Mol. Catal. B: Enzym.* **1998**, *5*, 137–141.
(7) Nagashima, S.; Nakasako, M.; Naoshi, D.; Tsujimura, M.; Takio, K.; Odaka, M.; Yohda, M.; Kamiya, N.; Endo, I. *Nat. Struct. Biol.* **1998**, *5*, 347–351.
(8) Huang, W.; Jia, J.; Cummings, J.; Nelson, M.; Schneider, G.; Lindqvist, Y. *Structure* **1997**, *5*, 691–699.
(9) Costas, M.; Mehn, M. P.; Jensen, M. P.; Que, L. J. *Chem. Rev.* **2004**, *104*, 939–986.
(10) Emerson, J. P.; Farquhar, E. R.; Que, L. *Angew. Chem., Int. Ed. Engl.* **2007**, *46*, 8553–8556.
(11) Pau, M. Y. M.; Lipscomb, J. D.; Solomon, E. *Proc. Natl. Acad. Sci. U.S.A.* **2007**, *104*, 18355–18362.
(12) Joseph, C. A.; Maroney, M. J. *Chem. Commun.* **2007**, 3338–3349.
(13) Kovacs, J. A. *Chem. Rev.* **2004**, *104*, 825–848.
(14) Kovacs, J. A.; Brines, L. M. *Acc. Chem. Res.* **2007**, *40*, 501–509.

10.1021/ic801704n CCC: $40.75
Published on Web 11/07/2008

acid[15] (^{114}Cys-S-OH)[1] or possibly ^{114}CyS-SO_2^- and the other to a sulfinate (^{112}CyS-SO_2^-).[16]

Our group has been attempting to determine how the unusual active site structure of NHase contributes to its function.[1,13,14,17−21] For example, why does nature incorporate cysteinates only to modify them? Is there a correlation between structure, spin state, and reactivity? What ligand environment is necessary for stabilization of a low-spin state? The low-spin state of NHase is unusual given that π-donor ligands, such as RS^-, usually favor a high-spin state.[20] The majority of nonheme iron enzymes are high spin,[9,11] and porphyrin ligands were originally thought to be necessary to stabilize low-spin Fe(III).[22] We and others have shown that the magnetic and spectroscopic properties of NHase can be accurately reproduced by six-coordinate Fe(III) model complexes[23−28] containing two *cis*-thiolates, imines, and in some cases an open binding site trans to one of the thiolates.[13,18,21,25,27] Detailed spectroscopic and theoretical studies involving some of these compounds have shown that anisotropy in the available π-symmetry metal orbitals contributes to stabilization of a low-spin state[20] as does the highly covalent nature of the Fe−S bonds.

The mechanism by which NHase operates has yet to be elucidated. It has been proposed that the iron site serves as either a hydroxide source or as a Lewis-acidic site to which nitriles coordinate.[4,8,16,26,29−36] In either case, the Fe^{3+} ion must be capable of binding H_2O, OH^-, or RCN. The tetraanionic $[N_2^{amide}S^{cys}(^{cys}SOH)(^{cys}SO_2)]^{4-}$ ligand environment of NHase would, however, be expected to decrease the metal ion Lewis acidity and affinity for substrates. The oxygen atoms and/or protons ^{cys}SOH and $^{cys}SO_2^-$, incorporated during post-translational modification, may help to offset this charge build up.[36] Insight regarding the functional role of the oxidized cysteinates would require isolation of the unmodified form of NHase. However, this form of the enzyme has yet to be characterized with a coordinated metal ion. An unmodified apo form of Co-type NHase has been structurally characterized and shown to contain a cysteine-disulfide in place of the post-translationally oxidized sulfurs (Figure 1).[37] However, in the absence of a metal ion, this structure does not indicate how the absence of oxygens might influence the electronic and reactivity properties important to function.

Figure 1. Post-translationally modified NHase active site.

Scheme 1

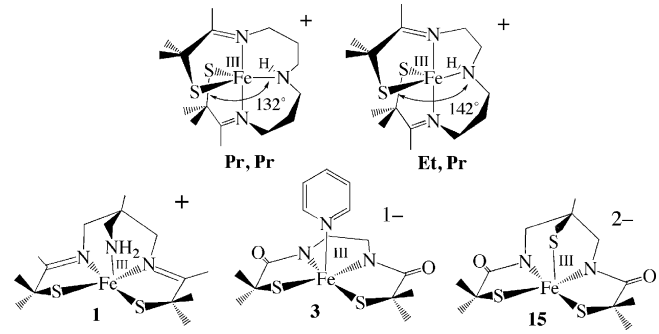

Previous NHase analogues synthesized by our group include five-coordinate $[Fe^{III}((Pr,Pr-N_3)S_2^{Me2})]^+$ (**Pr,Pr** in Scheme 1) and $[Fe^{III}((Et,Pr-N_3)S_2^{Me2})]^+$ (**Et,Pr** in Scheme 1) which bind NO and reversibly bind azide[38] but do not readily bind nitriles at ambient temperature.[18] The reactivity of these models was shown to correlate with spin state.[18,21,38,39] Ligand constraints and metal ion accessibility may also limit reactivity given that the pentadentate **Pr,Pr** and **Et,Pr** ligands favor trigonal-bipyramidal over octahedral geometries.[13,14] These ligands also incorporate a less anionic ligand set relative to that found at the active site of NHase. This prompted us to look into the design of models with less constraining ligands, a more open face, and deprotonated carboxamides in place of imines. Herein, we describe and

(15) Song, L.; Wang, M.; Shi, J.; Xue, Z.; Wang, M.-X.; Qian, S. *Biochem. Biophys. Res. Commun.* **2007**, *362*, 319–324.
(16) Nagashima, S. N., M.; Naoshi, D.; Tsujimura, M.; Takio, K.; Odaka, M.; Yohda, M.; Kamiya, N.; Endo, I. *Nat. Struct. Biol.* **1998**, *5*, 347–351.
(17) Lugo-Mas, P.; Dey, A.; Xu, L.; Davin, S. D.; Benedict, J.; Kaminsky, W.; Hodgson, K. O.; Hedman, B.; Solomon, E. I.; Kovacs, J. A. *J. Am. Chem. Soc.* **2006**, *128*, 11211–11221.
(18) Shearer, J.; Jackson, H. L.; Schweitzer, D.; Rittenberg, D. K.; Leavy, T. M.; Kaminsky, W.; Scarrow, R. C.; Kovacs, J. A. *J. Am. Chem. Soc.* **2002**, *124*, 11417–11428.
(19) Shearer, J.; Kung, I. Y.; Lovell, S.; Kaminsky, W.; Kovacs, J. A. *J. Am. Chem. Soc.* **2001**, *123*, 463–468.
(20) Kennepohl, P.; Neese, F.; Schweitzer, D.; Jackson, H. L.; Kovacs, J. A.; Solomon, E. I. *Inorg. Chem.* **2005**, *44*, 1826–1836.
(21) Ellison, J. J.; Nienstedt, A.; Shoner, S. C.; Barnhart, D.; Cowen, J. A.; Kovacs, J. A. *J. Am. Chem. Soc.* **1998**, *120*, 5691–5700.
(22) Frausto da Silva, J. J. R.; Williams, R. J. P. The Biological Chemistry of the Elements. *The Inorganic Chemistry of Life*, 2nd ed.; Oxford University Press: Oxford, 2001.
(23) Shoner, S.; Barnhart, D.; Kovacs, J. A. *Inorg. Chem.* **1995**, *34*, 4517–4518.
(24) Ellison, J. J.; Nienstedt, A.; Shoner, S. C.; Barnhart, D.; Cowen, J. A.; Kovacs, J. A. *J. Am. Chem. Soc.* **1998**, *120*, 5691–5700.
(25) Schweitzer, D.; Ellison, J. J.; Shoner, S. C.; Lovell, S.; Kovacs, J. A. *J. Am. Chem. Soc.* **1998**, *120*, 10996–10997.
(26) Scarrow, R. C.; Strickler, B.; Ellison, J. J.; Shoner, S. C.; Kovacs, J. A.; Cummings, J. G.; Nelson, M. J. *J. Am. Chem. Soc.* **1998**, *120*, 9237–9245.
(27) Mascharak, P. K.; Harrop, T. C. *Acc. Chem. Res.* **2004**, *37*, 253–260.
(28) Mascharak, P. K. *Coord. Chem.* **2002**, *225*, 201–214.
(29) Hopmann, K. H.; Himo, F. *Eur. J. Inorg. Chem.* **2008**, 1406–1412.
(30) Odaka, M.; Fujii, K.; Hoshino, M.; Noguchi, T.; Tsujimura, M.; Nagashima, S.; Yohada, N.; Nagamune, T.; Inoue, I.; Endo, I. *J. Am. Chem. Soc.* **1997**, *119*, 3785–3791.
(31) Scarrow, R. C.; Brennan, B. A.; Nelson, M. J. *Biochemistry* **1996**, *35*, 10078–10088.
(32) Jin, H.; Turner, I. M., Jr.; Nelson, M. J.; Gurbiel, R. J.; Doan, P. E.; Hoffman, B. M. *J. Am. Chem. Soc.* **1993**, *115*, 5290–5291.
(33) Nelson, M. J.; Jin, H.; Turner, I. M., Jr.; Grove, G.; Scarrow, R. C.; Brennan, B. A.; Que, L., Jr *J. Am. Chem. Soc.* **1991**, *113*, 7072–7073.
(34) Brennan, B. A.; Cummings, J. G.; Chase, D. B.; Turner, I. M., Jr.; Nelson, M. J. *Biochemistry* **1996**, *35*, 10068–10077.
(35) Bonnet, D.; Artaud, I.; Moali, C.; Petre, D.; Mansuy, D. *FEBS Lett.* **1997**, *409*, 216–220.
(36) Greene, S. N.; Richards, N. G. J. *Inorg. Chem.* **2006**, *45*, 17–36.
(37) Miyanaga, A.; Fushinobu, S.; Ito, K.; Shoun, H.; Wakagi, T. *Eur. J. Biochem.* **2004**, *271*, 429–438.
(38) Schweitzer, D.; Shearer, J.; Rittenberg, D. K.; Shoner, S. C.; Ellison, J. J.; Loloee, R.; Lovell, S. C.; Barnhart, D. K.; Kovacs, J. A. *Inorg. Chem.* **2002**, *41*, 3128–3136.
(39) Lugo-Mas, P. T., W.; Schweitzer, D.; Theisen, R. M.; Xu, L.; Shearer, J.; DiPasquale, A.; Kaminsky, W.; Kovacs, J. A. **2008**, submitted for publication.

compare the structural and reactivity properties of three new square-pyramidal thiolate-ligated Fe(III) complexes with ligands that favor the orthogonal angles required for substrate binding and in one case an anionic bis-carboxamide, tris-thiolate N_2S_3 coordination sphere possibly matching that of the yet-to-be characterized unmodified form of NHase. In order to determine how anionic charge build up influences substrate affinity, structurally related cationic, anionic, and dianionic complexes are compared.

Results and Discussion

Syntheses of Thiolate-Ligated Model Complexes. Synthesis of transition-metal complexes containing an open coordination site usually requires use of steric bulk, noncoordinating solvents and strict avoidance of potentially coordinating counterions.[40−45] Isolation of coordinatively unsaturated monomeric complexes is especially difficult when thiolates are included in the coordination sphere since metal thiolates are prone to oligomerization.[46−48] When mimicking a metalloenzyme active site, multidentate ligands are generally required in order to maintain a somewhat rigid structure since the biologically important first-row transition-metal ions tend to be substitution labile.[22,49] Previously we and others showed that gem dimethyls adjacent to the sulfur can prevent dimerization of iron thiolates.[18,21,50−52] More recently we showed that thiolate ligands reduce metal ion Lewis acidity relative to alkoxides and amines and have a strong trans influence, thereby helping to maintain an open coordination site.[53] The previously reported tame-N_3 (1,1,1-triaminoethane)[54,55] ligand was used in this study as a scaffold for the new complexes since it favors a more open, less constrained, square-pyramidal or octahedral geometry as illustrated in Scheme 1. Details regarding the synthesis of the new tris-thiol, bis-carboxamide tame-$(NH)_2(SH)_3$ (**14**)

Scheme 2

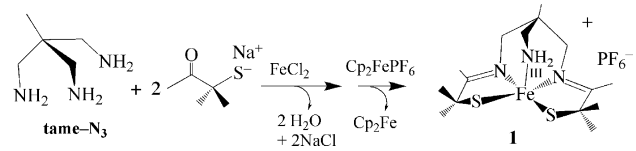

ligand as well as synthesis and crystallographic characterization of square-pyramidal $[Fe^{III}((tame\text{-}N_3)S_2^{Me2})](PF_6)\cdot PhCN$ (**1**), $(Me_4N)[Fe^{III}(Et\text{-}N_2S_2^{Me2})(Py)]\cdot 2MeOH$ (**3**), $(NMe_4)_2[Fe^{III}\text{-}((tame\text{-}N_2S)S_2^{Me2})]\cdot MeCN$ (**15**), and dimeric $(NMe_4)_2[Fe^{III}(Et\text{-}N_2S_2^{Me2})]_2\cdot 2MeOH$ (**2**) are provided in the Supporting Information.

Syntheses and Structure of Square-Pyramidal $[Fe^{II}\text{-}((tame\text{-}N_3)S_2^{Me2})]^+$ (1), $[Fe^{III}(Et\text{-}N_2S_2^{Me2})]_2^{2-}$ (2), $[Fe^{III}(Et\text{-}N_2S_2^{Me2})(py)]^{1-}$ (3), and $[Fe^{III}((tame\text{-}N_2S)S_2^{Me2})]^{2-}$ (15). Imine-ligated $[Fe^{III}((tame\text{-}N_3)S_2^{Me2})](PF_6)\cdot PhCN$ (**1**) was synthesized under anaerobic conditions via an Fe^{2+}-templated, Schiff-base condensation reaction between tame-N_3 and 2 equiv of deprotonated 3-methyl-3mercapto-2-butanone[24] followed by oxidation with Cp_2Fe^+ in benzonitrile (Scheme 2). The carboxamide-containing ligand *N*,*N*′-1,2-ethanediylbis[2-mercapto-2-methyl-propanamide] (Et-$(NH)_2(SH)_2^{Me2}$) was synthesized as described elsewhere,[56] and deprotonation in the presence of $(NMe_4)[FeCl_4]$ to initially afford a thiolate-bridged dimeric complex $(NMe_4)_2[Fe^{III}(Et\text{-}N_2S_2^{Me2})]_2\cdot 2MeOH$ (**2** Scheme 3, Figure 2), which is readily cleaved into monomers by coordinating solvents. Addition of excess pyridine to dimeric **2** in MeOH (2:1 MeOH/pyridine) results in cleavage of the bridging Fe(1)−S(3) and Fe(2)−S(1) bonds to afford monomeric, monoanionic pyridine-ligated $(Me_4N)[Fe^{III}(Et\text{-}N_2S_2^{Me2})(Py)]\cdot 2MeOH$ (**3**; Scheme 3, Figure 3). The protonated tris-thiol bis-carboxamide ligand tame-$(NH)_2(SH)_3$ (**14**) was synthesized in excellent yields according to the six-step convergent synthesis outlined in Scheme 4. This involves addition of $HBr_{(aq)}$ to 3-methyl-oxetan-3-yl-methanol (**5**) to afford diol **6** in 72% yield followed by SN_2 displacement of the bromine upon addition of deprotonated benzyl mercaptan to afford **7** in 98% yield. Conversion of diol **7** to diazide **8** was achieved via addition of DDQ/PPh_3/n-Bu_4NN_3. Reduction of **8** was achieved using PPh_3 to afford diamine **9** in 93% yield. This fragment is an analogue of the tame-N_3 ligand used in the synthesis of **1** (Scheme 2). To incorporate two more aliphatic thiolates into **14**, a second fragment (**12**) was synthesized via addition of benzyl mercaptan to ethyl 2-bromo-2-methyl propionate (**10**) in the presence of base to initially afford **11** (in 80% yield), which was converted to the chloride derivative **12** via addition of thionyl chloride. Addition of tame-derived **9** to **12** afforded benzyl-protected tris-thiolate **13**. Deprotection of the sulfurs using Na/NH_3 followed by addition of HCl afforded tame-$(NH)_2(SH)_3$ (**14**) (ESI-MS = 339.3, Figure

(40) Cramer, C. J.; Tolman, W. B. *Acc. Chem. Res.* **2007**, *40*, 601–608.
(41) Yandulov, D. V.; Schrock, R. R. *J. Am. Chem. Soc.* **2002**, *124*, 6252–6253.
(42) Smith, J. M.; Sadique, A. R.; Cundari, T. R.; Rodgers, K. R.; Lukat-Rodgers, G.; Lachicotte, R. J.; Flaschenriem, C. J.; Vela, J.; Holland, P. L. *J. Am. Chem. Soc.* **2006**, *128*, 756–769.
(43) O'Keefe, B. J.; Breyfogle, L. E.; Hillmyer, M. A.; Tolman, W. B. *J. Am. Chem. Soc.* **2002**, *124*, 4384–4393.
(44) Brown, S. D.; Betley, T. A.; Peters, J. C. *J. Am. Chem. Soc.* **2003**, *125*, 322–323.
(45) MacBeth, C. E.; Hammes, B. S.; Young, V. G.; Borovik, A. S. *Inorg. Chem.* **2001**, *40*, 4733–4741.
(46) Hagen, K. S.; Holm, R. H. *J. Am. Chem. Soc.* **1982**, *104*, 5496–5497.
(47) Millar, M.; Lee, J. F.; Koch, S. A.; Fikar, R. *Inorg. Chem.* **1982**, *21*, 4105–4106.
(48) Gebhard, M. S.; Deaton, J. C.; Koch, S. A.; Millar, M.; Solomon, E. I. *J. Am. Chem. Soc.* **1990**, *112*, 2217–2231.
(49) Lippard, S. J.; Berg, J. M. *Principles of Bioinorganic Chemistry*; University Science: Mill Valley, CA, 1994.
(50) Shoner, S. C.; Nienstedt, A.; Ellison, J. J.; Kung, I.; Barnhart, D.; Kovacs, J. A. *Inorg. Chem.* **1998**, *37*, 5721–5725.
(51) Krishnamurthy, D.; Sarjeant, A. N.; Goldberg, D. P.; Caneschi; Totti, F.; Zakharov, L. N.; Rheingold, A. L. *Chem. Eur. J.* **2005**, *11*, 7328–7341.
(52) Brines, L. M.; Shearer, J.; Fender, J. K.; Schweitzer, D.; Shoner, S. C.; Barnhart, D.; Kaminsky, W.; Lovell, S.; Kovacs, J. A. *Inorg. Chem.* **2007**, *46*, 9267–9277.
(53) Brines, L. M.; Villar-Acevedo, G.; Kitagawa, T.; Swartz, R. D.; Lugo-Mas, P.; Kaminsky, W.; Benedict, J. B.; Kovacs, J. A. *Inorg. Chim. Acta* **2008**, *361*, 1070–1078.
(54) Liu, S.; Wong, E.; Karunaratne, V.; Rettig, S. J.; Orvig, C. *Inorg. Chem.* **1993**, *32*, 1756–1765.
(55) Song, B.; Reuber, J.; Ochs, C.; Hahn, F. E.; Lugger, T.; Orvig, C. *Inorg. Chem.* **2001**, *40*, 1527–1535.
(56) Kruger, H. J.; Peng, G.; Holm, R. H. *Inorg. Chem.* **1991**, *30*, 734–742.

Scheme 3

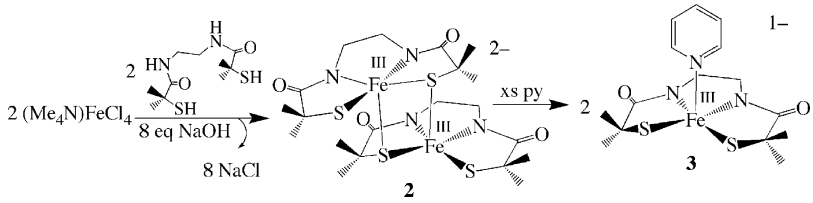

S-8, Supporting Information). Evidence for the presence of the free thiols was obtained by ^{1}H NMR (Figures S-5 and S-6, Supporting Information) and IR spectroscopy (ν_{SH} = 2544 cm^{-1}, Figure S-7, Supporting Information). The corresponding tris-thiolate-ligated Fe^{3+} complex $[Fe^{III}(tame\text{-}N_2S)S_2^{Me2})]^{2-}$ (**15**) was synthesized via addition of 5 equiv of NaOMe to a mixture of tame-$(NH)_2(SH)_3$ (**14**) and $(Me_4N)FeCl_4$ in MeOH at −35 °C.

X-ray quality crystals of **1**, dimeric **2**, and monomeric **3** were obtained by layering Et_2O onto concentrated PhCN, MeOH, and 2:1 MeOH/pyridine solutions, respectively, and cooling to −35 °C. X-ray-quality crystals of $(NMe_4)_2[Fe^{III}((tame\text{-}N_2S)S_2^{Me2})]\cdot$MeCN (**15**) were obtained by layered diffusion of Et_2O into a MeCN solution at −35 °C. Crystallographic data collection and refinement parameters are contained in Table S-1, Supporting Information, and metrical parameters for complexes **1**−**3** are compared in Table S-2, Supporting Information. As shown in the ORTEP diagram of Figure 3, monomeric **1** contains a five-coordinate Fe^{3+} ion in a square-pyramidal geometry (τ = 0.0)[57] with two cis-thiolates and two cis-imine nitrogens (N(1) and N(1′)) in the basal plane and an apical primary amine nitrogen (N(2)). The square-pyramidal Fe^{3+} ions of **3** and **15**, on the other hand, contain two cis carboxamides (N(1) and N(2)) in place of **1**′s imines in combination with two cis thiolates in the N_2S_2 basal plane and either an apical pyridine (**3**) or a thiolate (**15**) in place of the primary amine (**1**). The Fe^{3+} ion of **1** sits 0.293 Å above the mean basal N_2S_2 plane and on a crystallographic mirror plane, rendering S(1) and S(1′) as well as N(1) and N(1′) equivalent. The Fe^{3+} ion of **3** and **15**, on the other hand, is pulled further (0.404 Å with **3** and 0.408 Å with **15**) above the mean basal N_2S_2 plane, indicating that the metal ion has a higher affinity for apical thiolate and pyridine ligands. The N_3S_2 and N_2S_3 coordination spheres of **3** (τ = 0.090) and **15** (τ = 0.16) deviate only slightly from ideal square pyramidal (τ = 0.0).[57] The tris-thiolate, bis-carboxamide $[N_2S_3]^{5-}$ coordination sphere of **15** is potentially similar to that of the yet-to-be characterized unmodified form of NHase. The Fe^{3+} ions of **2** (Figure 2) sit 0.449 and 0.447 Å above the mean N_2S_2 basal planes each in an N_2S_3 coordination sphere that deviates only slightly (τ = 0.011 Å) from ideal square pyramidal. The basal plane Fe−S(1) distance of **1** (2.189(2) Å; Table S-2, Supporting Information) is noticeably shorter than those of **3** (2.21(1) Å) and **15** (2.22(2) Å), reflecting the stronger trans influence of carboxamide versus imine ligands. This bond is considerably shorter than the sum of the covalent radii (2.27Å),[58] indicating that the Fe−S bonds of **1** possess partial double-bond (or significant ionic) character. The Fe−S bonds of dimeric **2** are differentiated by the distinct roles played by the sulfurs as terminal (S(2); Fe(1)−S(2) = 2.199(2) Å) versus bridging (S(1); Fe(1)−S(1) = 2.251(2) Å) ligands.

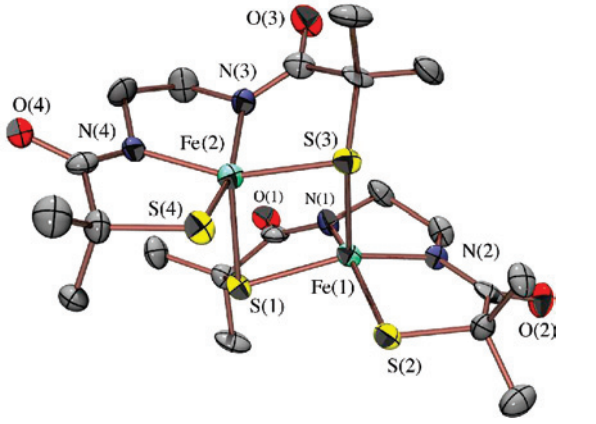

Figure 2. ORTEP diagram of the anion of dimeric $(NMe_4)_2[Fe^{III}((Et\text{-}N_2)S_2^{Me2})]_2\cdot$2MeOH (**2**) showing atom-labeling scheme. All hydrogen atoms have been removed for clarity.

Scheme 4

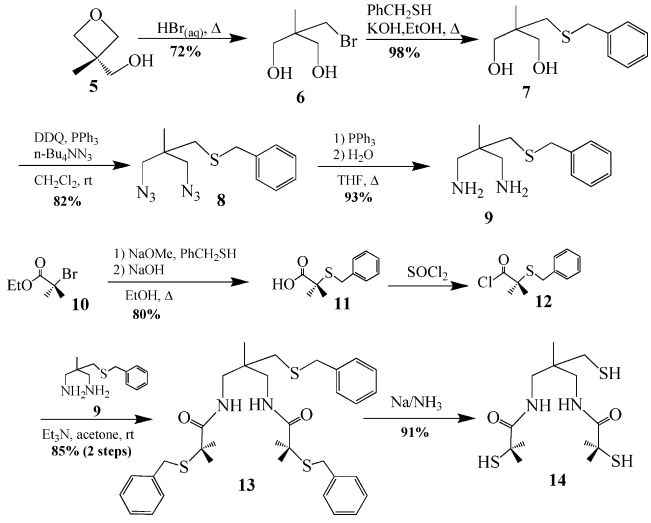

The apical Fe−X (X = primary amine (**1**), pyridine (**3**), and thiolate (**2** and **15**)) bonds are considerably longer than typical bonds of this type and/or the corresponding basal plane bonds. For example, Fe−N(amine) bonds usually fall in the range 2.0−2.06 Å,[17,21,59−62] A whereas the Fe−N(2) bond of **1** is longer (2.132(6) Å). Iron−pyridine Fe−N distances usually fall in the range of 1.92−2.14,[59,63−68] whereas that of **3** (Fe−N(3)) is longer (2.167(3) Å). The longer apical pyridine Fe−N(3) distance of **3** versus the

(57) Addison, A. W.; Rao, T. N.; Reedijk, J. *J. Chem. Soc., Dalton Trans.* **1984**, 1349.
(58) Pauling, L. *The Nature of the Chemical Bond*, 3rd ed.; Cornell University Press: Ithaca, NY, 1960.

Table 1. Electronic Absorption and Magnetic Properties of $S = 3/2$ Square-Pyramidal Fe^{III}−Thiolates versus $S = 1/2$ Complexes and NHase

compound	color	$\lambda_{max}(\epsilon)^a$(nm)	X-band EPR (g values)^b
$[Fe^{III}((tame\text{-}N_3)S_2^{Me2})]^+$ (**1**)	red	400(3380), 540(1300)	4.88, 2.60, 1.71
$[Fe^{III}(Et\text{-}N_2S_2^{Me2})]_2^{2-}$ (**2**)	red	306(7500), 497(3000) 420(5700), 465(6000)^c 320(9200), 497(3200)^e	4.35, 2.00
$[Fe^{III}(Et\text{-}N_2S_2^{Me2})(Py)]^{1-}$ (**3**)	red/brown	415(2600), 494(4800)^d 424(2600), 487(4800)^e	4.45, 1.97
$[Fe^{III}((tame\text{-}N_2S)S_2^{Me2})]^{2-}$ (**15**)	orange	471(3250), 433(2540, sh)	4.60, 3.40, 1.97
$[Fe^{III}(ADIT)_2]^+$	green	416(4200), 718(1400)	2.19, 2.13, 2.01
$[Fe^{III}(DITpy)_2]^+$	green	784(1300)	2.16, 2.10, 2.02
$[Fe^{III}(DITIm)_2]^+$	green	802(1300)	2.19, 2.15, 2.01
$[Fe^{III}((Pr,Pr)\text{-}N_3S_2^{Me2})(N_3)]^+$	green	460(220), 708(1600)	2.23, 2.16, 1.99
$[Fe^{III}((Et,Pr)\text{-}N_3S_2^{Me2})(MeCN)]^+$	green	454(∼1100), 833(∼1000)	2.17, 2.14, 2.01
NHase enzyme	green	710(∼1200)	2.27, 2.14, 1.97

^{a} In MeCN unless otherwise indicated. ^{b} In MeOH/EtOH (9:1) glass unless otherwise indicated. ^{c} Spectrum recorded in MeOH solution. ^{d} Spectrum recorded in pyridine solution. ^{e} Spectrum recorded in CH_2Cl_2 solution.

apical amine Fe−N(2) distance of **1** reflects the stronger basal ligand field imposed by the carboxamides as well as the decreased Lewis acidity of the metal ion caused by replacement of two neutral imines with two anionic deprotonated carboxamides. It is also possible that ligand constraints compress the apical amine distance. Pyridine Fe−N bonds are usually shorter, rather than longer, than amine Fe−N bonds. The apical Fe−S bonds in **2** (Fe−S(3) = 2.446(2) Å) and **15** (2.4058(7) Å) are considerably longer than the typical range (2.14−2.25 Å (low spin); 2.30−2.37 Å high spin),[17,23,24,38,59−62,67−70] reflecting a large differential between the apical and the basal ligand fields. This is supported by the magnetic data (vide infra) and indicates that in the case of **2** the thiolate bridge should readily cleave. Both the strong basal ligand field and the progressive negative charge build up (in going from cationic **1**, to monanionic **3**, and dianionic **15**) appear, therefore, to reduce the metal ion Lewis acidity of these square-pyramidal complexes and their affinity for built-in apical ligands. This is not without precedent given that deprotonated carboxamide ligands have been previously shown to favor lower coordination numbers.[71] In addition, we recently showed that when compared to alkoxides or amines, thiolate ligands favor lower coordination numbers.[53]

Electronic and Magnetic Properties. As illustrated in Table 1 the electronic and magnetic properties of the square-pyramidal compounds described herein differ notably from those of low-spin ($S = 1/2$) NHase and low-spin synthetic analogues described previously by our group.[1,13,14,17,18,20,21,23,59] All of the compounds described herein are intermediate-spin $S = 3/2$, and solutions appear various shades of red, whereas all of the low-spin complexes in Table 1 appear green. One can attribute these differences to changes in coordination number and the resulting decrease in the separation between energy states. The electronic spectrum of dimeric **2** is solvent dependent (Table 1). Coordinating solvents appear to cleave the dimer to afford solvent-bound five-coordinate derivatives based on a similarity of their spectra to that of pyridine-bound **3**. Six equivalents of pyridine are required to completely convert **2** to **3** in CH_2Cl_2 (Figure S-12, Supporting Information). In MeOH, the two Fe^{3+} ions of **2** behave independently, showing no signs of antiferromagnetic coupling, as indicated by the solution magnetic moment (μ_{eff}(298 K)/Fe^{3+} = 4.01 μ_B) and EPR spectrum ($g = 4.35, 2.00$, $E/D = 0.092$, Figure S-14, Supporting Information), which are consistent with a pure $S = 3/2$ spin state over all temperatures (5−298 K) examined. Monomeric **3** and **15** are also intermediate-spin $S = 3/2$ both in solution (μ_{eff}(**3**, 298 K, MeOH) = 3.72 μ_B; μ_{eff}(**15**, 298 K, MeOH) = 3.99 μ_B) and in the solid state (Figure 4) over all temperatures (4−300 K) examined. Fits to the low-temperature EPR data of **3** (Figure S-13, Supporting Information) and **15** (Figure 5) are consistent with an $S = 3/2$ ground state and Fe^{3+} in ∼axial (E/D 0.065) and slightly rhombic ($E/D = 0.107$) environments, respectively. Monomeric$[Fe^{III}(tame\text{-}N_3)S_2^{Me2})]^+$ (**1**) is also intermediate spin ($S = 3/2$) both in the solid state over the temperature range 7−300 K (μ_{eff} = 3.96 μ_B; Figure S-15, Supporting Information) and in MeOH solution (μ_{eff} = 3.74 μ_B) at ambient temperatures. Fits to the low-temperature (7 K) EPR data for **1** in noncoordinating solvents (e.g., 2-Me-THF) are consistent with Fe^{3+} in a rhombically distorted environment ($E/D = 0.185$) and a pure $S = 3/2$ ground state ($g = 4.88, 2.60, 1.71$; Figure S-16, Supporting Information). The only exception to these trends occurs in coordinating solvents at extremely low temperatures (7 K), where **1** is present as a mixture of $S = 1/2$ and 3/2 spin states ($g = 5.01, 4.25$ and $g = 2.25, 2.17, 1.95$; Figure S-17, Supporting Information).

(59) Jackson, H. L.; Shoner, S. C.; Rittenberg, D.; Cowen, J. A.; Lovell, S.; Barnhart, D.; Kovacs, J. A. *Inorg. Chem.* **2001**, *40*, 1646–1653.
(60) Shearer, J.; Fitch, S. B.; Kaminsky, W.; Benedict, J.; Scarrow, R. C.; Kovacs, J. A. *Proc. Natl. Acad. Sci., U.S.A.* **2003**, *100*, 3671–3676.
(61) Shearer, J.; Nehring, J.; Kaminsky, W.; Kovacs, J. A. *Inorg. Chem.* **2001**, *40*, 5483–5484.
(62) Schweitzer, D.; Ellison, J. J.; Shoner, S. C.; Lovell, S.; Kovacs, J. A. *J. Am. Chem. Soc.* **1998**, *120*, 10996–10997.
(63) Roelfes, G.; Lubben, M.; Chen, K.; Ho, R. Y. N.; Meetsma, A.; Genseberger, S.; Hermant, R. M.; Hage, R.; Mandal, S. K.; Young, V. G.; Zang, Y.; Kooijman, H.; Spek, A. L.; Que, L., Jr; Feringa, B. L. *Inorg. Chem.* **1999**, *38*, 1929–1936.
(64) Zang, Y.; Kim, J.; Dong, Y.; Wilkinson, E. C.; Appelman, E. H.; Que, L., Jr *J. Am. Chem. Soc.* **1997**, *119*, 4197–4205.
(65) Roelfes, G.; Lubben, M.; Chen, K.; Ho, R. Y. N.; Mettsma, A.; Genseberger, S.; Hermant, R. M.; Hage, R.; Mandal, S. K.; Young, V. G., Jr.; Zang, Y.; Kooijman, H.; Spek, A. L.; Que, L., Jr.; Feringa, B. L. *Inorg. Chem.* **1999**, *38*, 1929–1936.
(66) Marlin, D. S.; Olmstead, M. M.; Mascharak, P. K. *Inorg. Chem.* **1999**, *38*, 3258–3260.
(67) Noveron, J. C.; Olmstead, M. M.; Mascharak, P. K. *Inorg. Chem.* **1998**, *37*, 1138–1139.
(68) Noveron, J. C.; Olmstead, M. M.; Mascharak, P. K. *J. Am. Chem. Soc.* **2001**, *123*, 3247–3259.
(69) Theisen, R. M.; Shearer, J.; Kaminsky, W.; Kovacs, J. A. *Inorg. Chem.* **2004**, *43*, 7682–7690.
(70) Tyler, L. A.; Noveron, J. C.; Olmstead, M. M.; Mascharak, P. K. *Inorg. Chem.* **1999**, *38*, 616–617.
(71) Collins, T. J. *Acc. Chem. Res.* **1994**, *27*, 279.

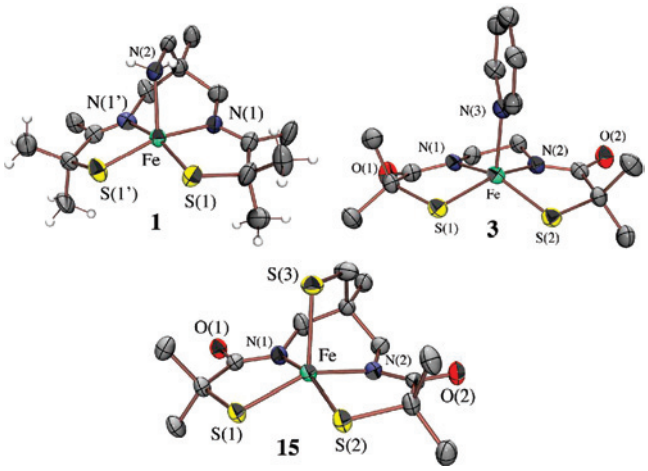

Figure 3. ORTEP diagram of the cation of $[Fe^{III}((tame\text{-}N_3)S_2^{Me2})](PF_6)\cdot PhCN$ (**1**) and the anions of $(Me_4N)[Fe^{III}((Et\text{-}N_2)S_2^{Me2})(Py)]\cdot 2MeOH$ (**3**) and $(NMe_4)_2[Fe^{III}((tameN_2S)S_2^{Me2})]\cdot MeCN$ (**15**) showing 50% ellipsoids and atom-labeling scheme. All hydrogen atoms have been removed for clarity.

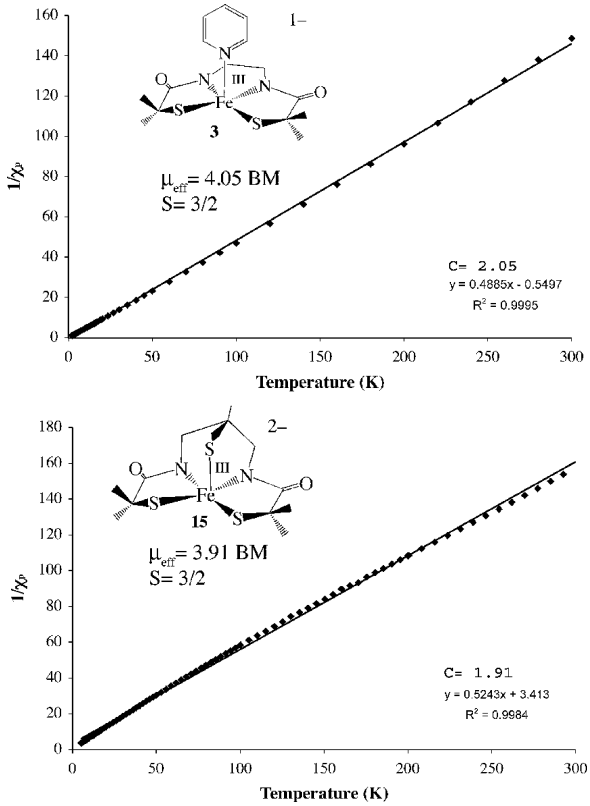

Figure 4. Inverse molar magnetic susceptibility $1/\chi_{:m}$ vs temperature (T) plot for $(Me_4N)[Fe^{III}((Et\text{-}N_2)S_2^{Me2})(Py)]\cdot 2MeOH$ (**3**) and $(NMe_4)_2[Fe^{III}((tame\text{-}N_2S)S_2^{Me2})]\cdot MeCN$ (**15**) each fit to an $S = 3/2$ spin state with Curie constants 2.05 (**3**) and 1.91 (**15**).

This would suggest that coordinating solvents bind to **1** at extremely low temperatures, where it would be entropically favored. The majority of characterized six-coordinate Fe^{III}−thiolates are low-spin $S = 1/2$, whereas five-coordinate Fe^{III}−thiolates tend to display temperature-dependent magnetic properties highly dependent upon geometry and S−Fe−S bond angles.[18,21,38,39] Solvent binding would raise the energy of the half-occupied d_{z^2} orbital of intermediate-spin **1**, causing the electron to drop into the t_{2g} set of orbitals resulting in an

Table 2. Redox Potential Dependence on Ligand Environment and Molecular Charge

compound	reduction potential (vs SCE), mV
$[Fe^{III}((tame\text{-}N_3)S_2^{Me2})]^+$ (**1**)	−650
$[Fe^{III}(DITIm)_2]^+$	−680
$[Fe^{III}(DITpy)_2]^+$	−930
$[Fe^{III}(ADIT)_2]^+$	−1002
$[Fe^{III}(Et\text{-}N_2S_2^{Me2})]_2^{2-}$ (**2**)	−1130
$[Fe^{III}(Et\text{-}N_2S_2^{Me2})(Py)]^{1-}$ (**3**)	−1340
$[Fe^{III}((tame\text{-}N_2S)S_2^{Me2})]^{2-}$ (**15**)	<−1800

$S = 3/2 \rightarrow 1/2$ spin-state change. In fact, when **1** is recrystallized from MeCN, a cocrystallized MeCN points toward the vacant site and appears to perturb the coordination environment at the Fe center, as determined by X-ray crystallography (vide infra); however, the complex remains intermediate spin at temperatures above 7 K.

Pure intermediate ($S = 3/2$) spin states of iron(III) are rare and predominantly seen when Fe^{3+} is in a tetragonally distorted environment in which the apical and equatorial ligand fields are dramatically different.[72−75] Dithiolenes, tetra-aza-macrocycles, and carboxamide ligands, for example, have all been shown to favor these spin states.[76−79] The relative stabilities of the $S = 3/2$ and 1/2 electronic configurations depend on the separation between the d_{xy} and d_{z^2} orbitals, ΔE (t_{2g}/e_g*) (Figure S-18, Supporting Information). Extensive π bonding with the thiolates and/or carboxamides in the xy plane of **1**, **3**, and **15** would push the d_{xy} orbital up in energy toward d_{z^2}, decreasing ΔE and thereby favoring an $S = 3/2$ ground state with a half-occupied d_{z^2} orbital. The half-occupied d_{z^2} orbital of an $S = 3/2$ spin system would decrease the open binding site's Lewis acidity relative to that of a low-spin ($S = 1/2$) system (Figure S-18, Supporting Information) with its empty d_{z^2} orbital. This could have important consequences when it comes to "substrate" binding (vide infra).

Redox Properties. As shown by the negative redox potentials of Table 2 and the cyclic voltammograms of Figures 6 and S-19, Supporting Information, the ligands described in this study stabilize iron in the +3 oxidation state, adhering to trends established for thiolate/carboxamide-ligated iron complexes.[13,14,23,27,59,67,68,80] Redox potentials shift in a negative direction as anionic carboxamides are incorporated in place of **1**'s neutral imines (Table 2)[81,82] as

(72) Keutel, H.; Käpplinger, I.; Jäger, E. G.; Grodzicki, M.; Schunemann, V.; Trautwein, A. X. *Inorg. Chem.* **1999**, *38*, 2320–2327.
(73) Fettouhi, M.; Morsy, M.; Waheed, A.; Golhen, S.; Ouahab, L.; Sutter, J.-P.; Kahn, O.; Menendez, N.; Varret, F. *Inorg. Chem.* **1999**, *38*, 4910–4912.
(74) Kostka, K. L.; Fox, B. G.; Hendrich, M. P.; Collins, T. J.; Rickard, C. E. F.; Wright, L. J.; Munck, E. *J. Am. Chem. Soc.* **1993**, *115*, 6746–6757.
(75) Simonato, J. P.; Pécaut, J.; Le Pape, L.; Oddou, J. L.; Jeandey, C.; Shang, M.; Scheidt, W. R.; Wojaczyński, J.; Wolowiec, S.; Latos-Grazyński, L.; Marchon, J. C. *Inorg. Chem.* **2000**, *39*, 3978–3987.
(76) Keutel, H.; Käpplinger, I.; Jäger, E. G.; Grodzicki, M.; Schunemann, V.; Trautwein, A. X. *Inorg. Chem.* **1999**, *38*, 2320–2327.
(77) Fettouhi, M.; Morsy, M.; Waheed, A.; Golhen, S.; Ouahab, L. *Inorg. Chem.* **1999**, *38*, 4910–4912.
(78) Kostka, K. L.; Fox, B. G.; Hendrich, M. P.; Collins, T. J.; Rickard, C. E. F.; Wright, L. J.; Munck, E. *J. Am. Chem. Soc.* **1993**, *115*, 6746–6757.
(79) Collins, T. J. *Acc. Chem. Res.* **1994**, *27*, 279–285.
(80) Harrop, T. C.; Olmstead, M. M.; Mascharak, P. K. *Inorg. Chem.* **2005**, *44*, 9527–9533.

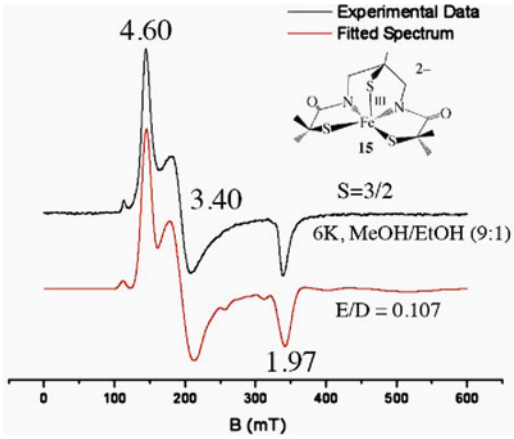

Figure 5. Low-temperature (6 K) X-band EPR spectrum (black) of $(NMe_4)_2[Fe^{III}((tame\text{-}N_2S)S_2^{Me2})]\cdot MeCN$ (**15**) in MeOH/EtOH (9:1) glass, fitted (red) to $E/D = 0.107$.

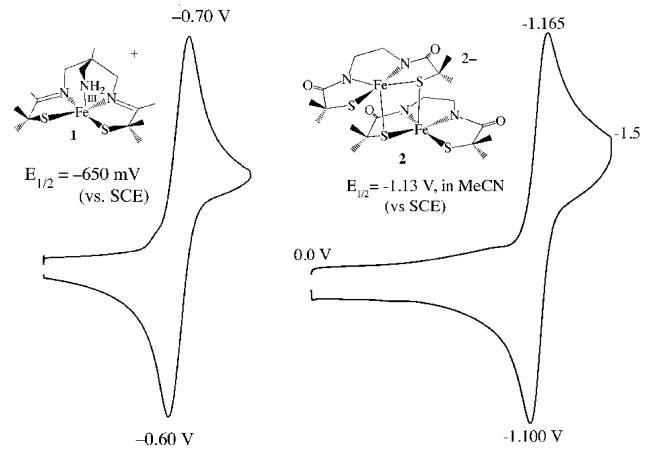

Figure 6. Cyclic voltammogram of $[Fe^{III}((tame\text{-}N_3)S_2^{Me2})](PF_6)\cdot PhCN$ (**1**) and $(NMe_4)_2[Fe^{III}((Et\text{-}N_2)S_2^{Me2})]_2\cdot 2MeOH$ (**2**) (both in MeCN at 298 K (0.1 M $(Bu_4N)PF_6$, glassy carbon electrode, 150 mV/s scan rate). Peak potentials versus SCE indicated.

well as when the neutral apical amine of **3** is replaced by an anionic apical thiolate in **15**. In fact, the 5− charge of **15**'s $[N_2S_3]^{5-}$ ligand creates such an electron-rich environment for the Fe^{3+} ion that no reduction wave is observed in the window +1.0 → −1.8 V (vs SCE). This shows that the +2 oxidation state is inaccessible at reasonable potentials and that the energy of the redox-active orbital is raised dramatically when Fe^{3+} is placed in an environment identical to that of unmodified NHase. The inaccessibility of the +2 oxidation state is important for prevention of undesirable Fenton-type side reactions.[83]

Reactivity of Five-Coordinate $[Fe^{III}((tame\text{-}N_3)S_2^{Me2})]^+$ (1), $[Fe^{III}(Et\text{-}N_2S_2^{Me2})(Py)]^{1-}$ (3), and $[Fe^{III}((tame\text{-}N_2S)S_2^{Me2})]^{2-}$ (15), and dimeric $[Fe^{III}(Et\text{-}N_2S_2^{Me2})]_2^{2-}$ (2). Although dimeric $[Fe^{III}(Et\text{-}N_2S_2^{Me2})]_2^{2-}$ (**2**) undergoes bridge cleavage reactions with neutral ligands such as pyridine, the resulting $S = 3/2$ anionic compound $[Fe^{III}(Et\text{-}N_2S_2^{Me2})(Py)]^{1-}$ (**3**) remains five coordinate even in neat pyridine. Dianionic $S = 3/2$ $[Fe^{III}(tame\text{-}N_2S)S_2^{Me2})]^{2-}$ (**15**) displays a similar lack of affinity for additional ligands. Even when added in excess (>100 equiv) and at low temperatures (−78 °C), anionic (N_3^-, CN^-), neutral (py, CO), and/or σ-donor ligands (MeCN) show no signs of binding to **3** or **15**, as determined by electronic absorption spectroscopy. Nitric oxide reacts with **15**; however, the product obtained in this reaction proved to be too unstable to isolate. Cationic $S = 3/2$ $[Fe^{III}((tame\text{-}N_3)S_2^{Me2})]^+$ (**1**) is only slightly more reactive than anionic **3** and **15**, suggesting that overall molecular charge (1− vs 1+) and the weaker ligand field (imines in **1** versus carboxamides in **3** and **15**) only slightly influence reactivity properties. Cationic **1** will only bind π-acid ligands such as NO at ambient temperature and not anions such as CN^- or N_3^-. Neutral ligands (such as MeOH) bind to cationic **1** only at extremely low (7 K) temperatures (vide supra). At 7 K anionic **3** and **15**, on the other hand, show no signs (by EPR) of binding neutral ligands. Although oxidized **1** does not bind CO, its neutral reduced Fe(II) precursor can be trapped with CO(g), affording $[Fe^{II}((tame\text{-}N_3)S_2^{Me})(CO)]$ (**16**). The extremely low ν_{CO} stretch (1895 cm^{-1} (**16**; Figure S-20, Supporting Information) vs typical $Fe^{II}-CO$ range $\nu_{CO} = 1929-1969$ cm^{-1}) indicates that the Fe^{2+} ion of **16** is fairly electron rich. Carbonyl-ligated Fe^{2+} compounds are rare and typically quite labile.[24,84] For example, previously reported $[Fe^{II}((Pr,Pr)\text{-}N_3S_2^{Me2})(CO)]$ (**17**, $\nu_{CO} = 1929$ cm^{-1}) readily dissociates CO at temperatures above 0 °C.[24] Carbonyl-ligated **16** (Figure 7) is considerably more stable than **17**, most likely because CO binds trans to an amine in **16** as opposed to a thiolate in **17**. Quantitative addition of NO(g) to oxidized **1** affords $[Fe^{III}((tame\text{-}N_3)S_2^{Me})(NO)]^+$ (**18**), an analogue of the NO-inhibited form of NHase. Complex **18** (Figure 7) displays an ν_{NO} stretch (1865 cm^{-1}; Figure S-21, Supporting Information) close to that of NHase ($\nu_{NO} = 1853$ cm^{-1}) and is diamagnetic (Figure S-22, Supporting Information), indicating that NO radical binding induces a spin-state change at the metal $S = 3/2 \rightarrow 1/2$. The mean Fe−S distance in **18** (2.254(4) Å) is 0.068 Å longer than in **1** and 0.024 Å shorter than in reduced carbonyl-bound **16** (2.278(1) Å; Table S-3, Supporting Information), indicating that the most appropriate formal electronic description lies somewhere between $Fe(III)-NO^{\bullet}$ and $Fe(II)-NO^+$. Metrical parameters for **16** are compared with that of **18** in Table S-3, Supporting Information.

On the basis of the appearance of a new low-spin species in the EPR spectrum (Figure S-17, Supporting Information), cationic **1** does appear to bind neutral σ donors such as MeOH but only at extremely low temperatures (7 K). When MeCN is used as the solvent for recrystallization of **1**, in place of PhCN, a cocrystallized MeCN points toward the vacant site of $[Fe^{III}(tame\text{-}N_3)S_2^{Me2})(MeCN)]^+$ (**19**) (Figure 7). Although this interaction is extremely weak (Fe−N(4) = 2.63 Å) it does appear to elongate the apical Fe−N(3) bond (by 0.056 Å in **19** relative to **1**; Tables S-2 and S-3, Supporting Information) and causes the Fe^{3+} ion to move 0.147 Å closer to the N_2S_2 basal plane (from 0.293 Å in **1** to 0.147 Å in **19**) away from apical amine N(3) toward the

(81) Kruger, H. J.; Holm, R. H. *J. Am. Chem. Soc.* **1990**, *112*, 2955–2963.
(82) Kruger, H. J.; Peng, G.; Holm, R. H. *Inorg. Chem.* **1991**, *30*, 734–742.
(83) Meyerstein, D.; Goldstein, S. *Acc. Chem. Res.* **1999**, *32*, 547–550.
(84) Nguyen, D. H.; Hsu, H. F.; Munck, E.; Millar, M.; Koch, S. A. *J. Am. Chem. Soc.* **1996**, *118*, 8963–8964.

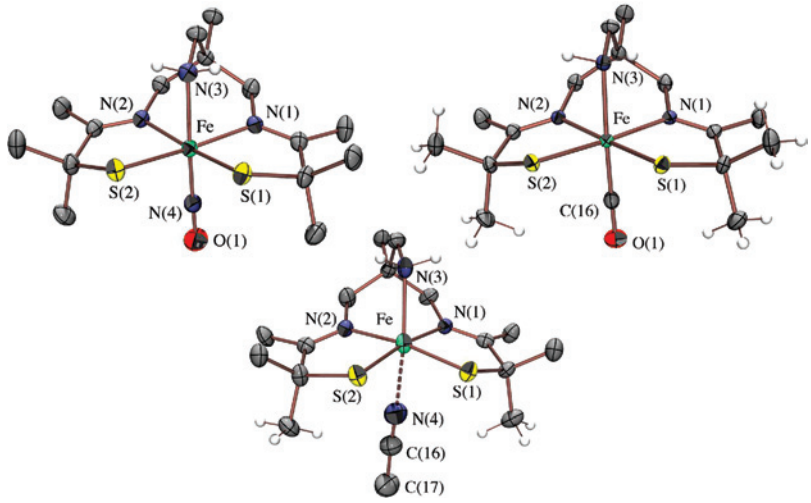

Figure 7. ORTEP diagram of reduced $[Fe^{II}((tame\text{-}N_3)S_2^{Me2})(CO)]\cdot MeCN$ (**16**) and the cations of $[Fe^{III}((tame\text{-}N_3)S_2^{Me2})(NO)](PF_6)$ (**18**) and $[Fe^{III}((tame\text{-}N_3)S_2^{Me2})(MeCN)](PF_6)\cdot MeCN$ (**19**) showing 50% ellipsoids and atom-labeling scheme as well as the weakly interacting MeCN (Fe−N(4) = 2.63 Å) in **19**.

acetonitrile (N(4)). The ν_{CN} (MeCN) value of 2254 cm^{-1} is close to that of free MeCN, and there is no significant increase in the nitrile C(16)−N(4) bond length in **19** (1.159(7) Å) relative to free MeCN (1.14 Å), indicating that the nitrile is by no means activated by its interaction with the Fe^{3+} ion.

Although the curtailed affinity of **3** and **15** for additional ligands could reflect the anionic charge, it could also reflect the presence of an electron in the intermediate-spin apical site orbital (vide supra; Figure S-18, Supporting Information). Reactivity has previously been shown by our group to correlate with spin state.[18,38,18,21,38,39] For example, low-spin (S = 1/2) five-coordinate $[Fe^{III}((Et,Pr)\text{-}N_3S_2^{Me2})]^+$ (**Et,Pr**; Scheme 1) binds a wide variety of ligands including nitriles (RCN, R = Me, Bz, Et, ^{t}Bu), py, ^{t}BuNC, MeOH, and $MeC(O)NH_2$) as well as N_3^- and NO.[18,38] Intermediate-spin (S = 3/2) five-coordinate $[Fe^{III}((Pr,Pr)\text{-}N^{Me}N_2^{amide}S_2^{Me2})]^{1-}$, on the other hand, does not appear to bind any of these ligands even at low temperatures.[39] Five-coordinate $[Fe^{II}((Pr,Pr)\text{-}N_3S_2^{Me2})]^+$ (**Pr,Pr**; Scheme 1) does not bind N_3^- at ambient temperatures where an S = 3/2 excited state is 23% populated but does at low temperatures (−80 °C) where an S = 1/2 state is predominantly populated.[18] The equilibrium for binding azide favors the azide-bound form of **Et,Pr** ($[Fe^{III}((Et,Pr)N_3S_2^{Me2})(N_3)]$) 10 times more than that of **Pr,Pr** ($[Fe^{III}((Pr,Pr)N_3S_2^{Me2})(N_3)]$),[38] meaning that an additional 2.3 kcal mol^{-1} energy is released when azide binds to low-spin (S = 1/2) **Et,Pr** versus partially (23%) intermediate-spin S = 3/2 **Pr,Pr**.

Given the potential similarity between $[Fe^{III}(tame\text{-}N_2S)S_2^{Me2})]^{2-}$ (**15**) and the uncharacterized unmodified form of NHase, the curtailed reactivity of the former suggests that post-translational oxygenation of the equatorial cysteinate sulfurs plays an important role in promoting substrate binding. This is supported by theoretical (DFT) calculations,[1] which predict that the hypothetical unmodified form of NHase has a weak affinity for water ($Fe-OH_2$ = 3.4 Å) unless the equatorial thiolate ligands are oxidized ($Fe-OH_2$ = 2.1 Å). Whereas the catalytically active, post-translationally modified form of NHase readily binds N_3^-, CN^-, and NO and hydrolyzes RCN our unmodified NHase analogue **15** does not bind substrates (RCN) or inhibitors (N_3^-, CN^-, or NO), even when present in excess and at low temperatures. H bonding may also play an important role in NHase activity, as suggested by the inactivity of mutants lacking highly conserved ^{56}Arg and ^{141}Arg.[85,86] In order to address the possible roles of thiolate oxidation and/or H bonding on reactivity we attempted to both oxidize the equatorial sulfurs of **15** and crystallize **15** in the presence of H-bond donors such as H_2O.

Unmodified NHase analogue **15** is soluble and stable in H_2O. Crystallization from "wet" DMF affords a structure containing two dianionic iron complexes $(NEt_4)_2[Fe^{III}((tame\text{-}N_2S)S_2^{Me2})]\cdot 3H_2O$ (**15a**) and three H_2O's each H bonded to a different carboxamide oxygen ($O(1)\cdots H(52)(H_2O)$ = 2.010 Å; O(1)−H(52)−O(5) = 163.3°; $O(2)\cdots H(72)(H_2O)$ = 2.049 Å; O(2)−H(72)−O(7) = 176.1°; $O(3)\cdots H(61)(H_2O)$ = 1.998 Å; O(3)−H(61)−O(6) = 169.0°; Figure S-23, Supporting Information). Comparison of the two structures (**15** versus $\mathbf{15}\cdot 3H_2O$) shows very little change in carboxamide C−N (mean distance = 1.339(2) Å in $\mathbf{15}\cdot 3H_2O$ versus 1.337(3) Å in **15**) and C=O (mean distance = 1.26(1) Å in $\mathbf{15}\cdot 3H_2O$ versus 1.255(3) Å in **15**) bond distances (Table 2). The H-bonded complex $\mathbf{15}\cdot 3H_2O$ (Figure S-23, Supporting Information) remains five-coordinate and intermediate-spin S = 3/2. This is true even when excess guanidinium·HCl is added as a potential H-bond donor and mimic for the conserved arginine residues,[86] suggesting that sulfur oxygenation plays a more important role than H bonding in determining magnetic and reactivity properties.

Reactivity of Unmodified NHase Analogue $[Fe^{III}((tame\text{-}N_2S)S_2^{Me2})]^{2-}$ (15) with Dioxygen. Addition of dry O_2 to $[Fe^{III}((tame\text{-}N_2S)S_2^{Me2})]^{2-}$ (**15**) in MeCN results in addition

(85) Piersma, S. R.; Nojiri, M.; Tsujimura, M.; Noguchi, T.; Odaka, M.; Yohda, M.; Inoue, Y.; Endo, I. *J. Inorg. Biochem.* **2000**, *80*, 283–288.
(86) Endo, I.; Nojiri, M.; Tsujimura, M.; Nakasako, M.; Nagashima, S.; Yohda, M.; Odaka, M. *J. Inorg. Biochem.* **2001**, *83*, 247–253.

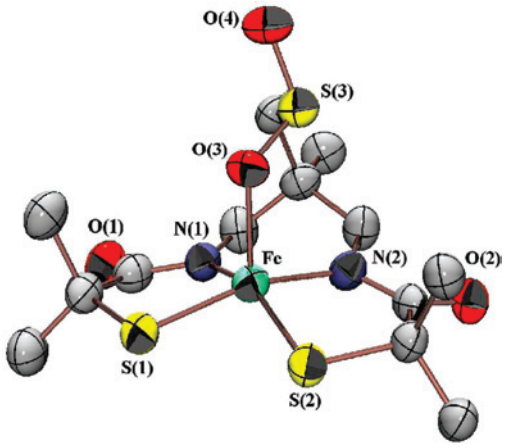

Figure 8. ORTEP diagram of the anion of $(NEt_4)_2[Fe^{III}((tame\text{-}N_2SO_2)S_2^{Me2})]\cdot MeCN$ (**20**) showing 50% ellipsoids and atom-labeling scheme.

of two oxygen atoms to the parent molecule as determined by ESI-MS. X-ray quality crystals of this oxygenated product were obtained upon low-temperature (−35 °C) layering of Et_2O onto an MeCN solution. As shown in the ORTEP diagram of Figure 8 the apical thiolate sulfur is selectively oxidized by O_2 to afford *O*-bound sulfinate-ligated $[Fe^{II}((tame\text{-}N_2SO_2)S_2^{Me2})]^{2-}$ (**20**). Preferential oxygenation of the apical sulfur occurs initially because the apical Fe−S(3) bond of 15 is significantly longer, making it the most basic sulfur and thus more susceptible to oxidation than the basal plane sulfurs S(1) and S(2). Rearrangement of this kinetic product to a potentially different thermodynamically preferred product would be expected to be slow since it would involve cleavage of fairly robust S=O bonds. Oxygenation of **15**'s apical sulfur not only leaves the $S = 3/2$ spin state ($\mu_{eff} = 3.75\ \mu_B$ (Figure S-24, Supporting Information); $g_\perp = 3.74$, $g_\parallel = 2.02$ (Figure S-25, Supporting Information)) and bond lengths (Table S-2, Supporting Information) unperturbed, but reactivity is unaffected as well. Like **15**, sulfinate-ligated **20** does not bind anionic (N_3^-, CN^-), neutral (Py, CO, NO), and/or σ-donor ligands (MeCN) even when added in excess (>100 equiv) and at low temperatures (−78 °C) as determined by electronic absorption spectroscopy. Given the similarity between **20** and the NHase active site, this implies that regioselective post-translational oxygenation of the basal plane sulfurs is critical to NHase function. In the enzyme, apical thiolate oxidation is prevented by its placement in a solvent-inaccessible site.[16] The basal plane sulfurs, on the other hand, point toward a solvent-accessible channel. Oxygenation of the basal sulfurs would weaken the basal plane ligand field by "tying up" the π-symmetry sulfur orbitals, increase the metal ion Lewis acidity, and thereby increase the apical Fe−S interaction[17] causing a spin-state change from $S = 3/2$ to 1/2 (Figure S-18, Supporting Information). The low-spin $S = 1/2$ state would possess a more Lewis-acidic d_{z^2} orbital that would more readily bind apical ligands.[87]

Summary and Conclusions

The strong N_2S_2 basal plane ligand field and anionic charge of equatorial carboxamides in the thiolate-ligated complexes described herein results in a significantly weakened apical ligand interaction even with tethered built-in ligands. Introduction of an apical thiolate in place of an amine does pull the Fe^{3+} ion out of the basal N_2S_2 plane however, indicating that it has a higher affinity for thiolates. Spin state may be responsible for reduced apical ligand affinity[18,87,88] since the intermediate $S = 3/2$ spin system, for all of the ligand-field combinations examined herein, would have an electron in the orbital (d_{z^2}) pointing toward the vacant site. This is in contrast to the post-translationally modified NHase active site, which is low spin with an empty apical site orbital and displays a higher affinity for apical ligands. Since the preferred ground state of six-coordinate iron thiolate complexes is $S = 1/2$,[13,14,23,59] "substrate" binding to an $S = 3/2$ spin system would require a spin-state change involving the pairing of electrons, and this could create an additional barrier to ligand binding. The mechanism by which NHase operates has yet to be elucidated. It has been proposed that the iron site serves as either a hydroxide source or a Lewis-acidic site to which nitriles coordinate.[4,8,16,26,29−36] Both mechanisms would require ligand binding to the vacant apical site. The results described herein suggest that regioselective post-translational oxygenation of the basal plane NHase cysteinates is required in order to weaken the equatorial ligand field and increase the Lewis acidity of the d_{z^2} orbital pointing toward the vacant apical site. Density functional calculations support this.[1]

Acknowledgment. This work was supported by the NIH (GM 45881). P.L.-M. gratefully acknowledges support by an NIH predoctoral minority fellowship (F31 GM73583-01).

Supporting Information Available: Experimental data for the tame-$(NH)_2$ $(SH)_3$ (**14**) ligand synthesis, including ESI mass spec, IR, and ^1H NMR data. Experimental and crystallographic data for complexes **1**−**3**, **15**, **15a**·$3H_2O$, **16**, and **18**−**20**; ORTEP diagram of **15a**·$3H_2O$; electronic absorption spectra of **1**−**3** and **15**; magnetic data for **1** and **20**; X-band EPR spectra of **1**−**3** and **20**; cyclic voltammogram of **3**; vibrational data for CO-bound **16** and NO-bound **18.** This material is available free of charge via the Internet at http://pubs.acs.org.

IC801704N

(87) Strickland, N.; Harvey, J. N. *J. Phys. Chem. B* **2007**, *111*, 841–852.
(88) Carreon-Macedo, J. L.; Harvey, J. N. *J. Am. Chem. Soc.* **2004**, *126*, 5789–5797.